Lactate Metabolism Regulates Tumour Growth and Progression in Glioblastoma

Lucia Longhitano
University of Catania
Nunzio Vicario
University of Catania
Daniele Tibullo (d.tibullo@unict.it)
Università degli Studi di Catania https://orcid.org/0000-0002-4416-8556
Cesarina Giallongo
University of Catania
Giuseppe Broggi
University of Catania
Rosario Caltabiano
University of Catania
Giuseppe Maria Vincenzo Barbagallo
University of Catania
Marta Baghini
University of Trento: Universita degli Studi di Trento
Michelino Di Rosa
University of Catania
Rosalba Parenti
University of Catania
Antonio Giordano
SHRO: Sbarro Health Research Organization
Maria Caterina Mione
University of Trento
Giovanni Li Volti
University of Catania

Research

Keywords: Lactate, glioblastoma, metabolism, MCT1, HCAR1

Posted Date: October 19th, 2021

DOI: https://doi.org/10.21203/rs.3.rs-965025/v1

Abstract

Background. Tumor microenvironment (TME) plays a pivotal role in establishing malignancy and it is associated with high glycolytic metabolism and increased lactate production accumulating in TME through monocarboxylate transporters (MCTs). Several lines of evidence suggest that lactate also serves as a signalling molecule through its receptor HCAR1thus functioning as a paracrine and autocrine signalling molecule in TME. The aim of the present study was to investigate the role of lactate in glioblastoma (GBM) progression and metabolic reprogramming in an in vitro and in vivo model.

Methods. Cell proliferation, migration and clonogenicity assay were performed in vitro on three different human GBM cell lines. Protein expression of MCT1, MCT4 and pharmacological lactate receptor (GPR81) were evaluated both in vitro and in a zebrafish GBM in vivo model. These results were further validated in patient-derived GBM biopsies.

Results. Our results showed that lactate significantly increased cell proliferation, migration and colony formation capacity of GBM cells, both in vitro and in vivo. We also showed that lactate increased MCT1 and HCAR1 expression. Moreover, lactate modulated epithelial-mesenchymal transition protein markers E-Cadherin and β-Catenin. Interestingly, lactate induced mitochondrial mass and OXPHOS gene suggesting an improved mitochondrial fitness. Similar effects were observed after treatment with 3,5-Dihydroxybenzoic acid, a known agonist of GPR81. Consistently, GBM zebrafish model exhibited an altered metabolism and increased expression of MCT1 and HCAR1 leading to high levels of extracellular lactate and thus supporting tumor cell proliferation. Our data from human GBM biopsies also showed that in high proliferative GBM biopsies, Ki67 positive cells expressed significantly higher levels of MCT1 compared to low proliferative GBM cells.

Conclusions. Our data suggest that lactate favours proliferation of neighbourhood cells by cooperating with their glycolytic metabolism, sensing and removing extracellular lactate. In particular, lactate and its transporter and receptor play a major role in GBM proliferation and migration thus representing a potential target to develop new strategies to counteract tumor progression and recurrencies.

Background

Glioblastoma (GBM) represents the most common primary brain tumor in the adult population and is classified by WHO as a grade IV glioma. Current therapeutic approach for newly diagnosed GBM relies on surgical resection, radiotherapy and chemotherapy (i.e. temozolomide) [1]. However, despite aggressive therapeutic regimens, these tumors still have a dismal prognosis with medial overall survival of 12 to 15 months. Histologically, GBM is a highly cellular glioma composed by glial cells with significant pleomorphism and nuclear atypia [2]. Such cellular features are coupled with microvascular proliferation and palisading necrosis characterized by regular areas of necrosis and dense accumulation of GBM cells [2]. GBM characteristics are related to cell proliferation, usually assessed by evaluating KI-67 expressing cells classifying high proliferative index (HPI, KI-67 positive cells > 30%) and low proliferative index (LPI,

KI-67 positive cells < 30%). Furthermore, GBM cell proliferation, migration and invasiveness are closely related to availability of blood-derived nutrients and oxygen. Indeed, two niches have been described in GBM in relation to availability of oxygen, the so-called perivascular niches, in which GBM cell receive glucose and oxygen from blood stream and oxidative phosphorylation in these cells determines highly efficient metabolism, and the GBM hypoxic niches, for example tumor core, in which low oxygen levels shapes metabolisms towards a glycolytic state inducing lactate accumulation [3]. Indeed, such tumors have a rapid rate of glucose consumption and convert large amounts of glucose into lactic acid, even in the presence of oxygen [4]. This metabolic phenotype, known as Warburg effect contrasts sharply with that observed in normal tissues in which glycolysis occurs mainly in hypoxic conditions [5].

To maintain enhanced glycolytic flow, glioblastomas require rapid outflow of lactic acid into the tumor microenvironment (TME), facilitated by a series of plasma membrane transporters called monocarboxylate transporters (MCTs) [6]; among these only four (MCT 1-4) are known to play a role in lactic acid transport in mammalian tissues, including cancers [7] and MCT1 and MCT4 have been implicated in multiple aspects of GBM progression including angiogenesis, cell proliferation and immunity modulation [8]. Glycolytic cancer cells are known to upregulate lactate export by increasing MCT4 expression to better adapt to lactate accumulation. In contrast, tumor cells of oxidative tumors have been reported to upregulate MCT1 expression to mediate lactate uptake from the extracellular environment to fuel metabolism [9]. A recent report suggests that this dynamic may create a metabolic symbiosis between the two GBM subpopulations maintaining a favorable environment for both subtypes [8, 10].

Besides having a role as end-product metabolite of glycolysis and being utilized by cellular metabolic programs to produce energy, lactate also acts as signalling molecule through its receptor HCAR1 (GPR81) [11]. Therefore, extracellular lactate is not a simple bystander causing milieu acidification but it also serves as a paracrine and autocrine signalling molecule in TME [12]. Elevated expression of HCAR1/GPR81 was found in carcinomas of the breast, pancreas and cervix, despite negligible expression in the corresponding benign epithelium [12, 13]. Several groups have identified autocrine roles for HCAR1/GPR81 in TME, where lactate produced by tumor cells activates HCAR1/GPR81 and confers cancer-promoting phenotypes [14], including upregulation of transporter MCT1 and MCT4 and the secretion of factors that promote angiogenesis and tumor progression [15].

The aim of the present study was to assess the role of lactate metabolism in cancer growth and progression in several glioblastoma cell lines, in pathological specimens and in an in vivo model.

Materials And Methods

GBM cell lines

Human glioblastoma cell lines (U87-MG, A172 and U251) were purchased from ATCC Company (Milan, Italy). Cells were suspended in DMEM (Gibco, cat. no. 11965092) culture medium containing 10% fetal bovine serum (FBS, Gibco, cat. no. 10082147), 100 U/mL penicillin and 100 U/mL streptomycin (Gibco,

cat. no. 15070063). At 80% confluency, cells were passaged using trypsin-EDTA solution (0.05% trypsin and 0.02% EDTA, Gibco, cat. no. 25300054).

Lactate (Sigma–Aldrich, Milan, Italy) and 3,5-Dihydroxybenzoic acid (Sigma–Aldrich, Milan, Italy) were added to cell culture of all experiments at final concentrations of 20 mM and 150 uM, respectively, for 24, 48 and 72 hours.

Clonogenic assay

Colony assays performed by seeding cells in 6-well plates at low density (2000 cells/well) and allowing growth for 10 days. Colonies were fixed, stained with crystal violet and colonies were quantified with Operetta high content screening (HCS) System (Perkin Elmer). The experiments were done in quadruplicates.

Real-Time Monitoring of Cell Proliferation

xCELLigence experiments were performed using the RTCA (Real-Time Cell Analyser) DP (Dual Plate) instrument according to manufacturers' instructions (Roche Applied Science, Mannheim, Germany and ACEA Biosciences, San Diego, CA). The RTCA DP Instrument includes three main components: (i) RTCA DP Analyser, which is placed inside a humidified incubator maintained at 37°C and 5% CO2, (ii) RTCA Control Unit with RTCA Software preinstalled and (iii) E-Plate 16 for proliferation assay. First, the optimal seeding number was determined by cell titration and growth experiments. After seeding the optimal cell number (3000 cells/well), cells were treated and automatically monitored every 15 min for 24h. Optimal cell number was determined in a preliminary set of experiments (data not shown) to obtain a significant cell index value and a constant cell growth during the entire duration of the experiment.

Cell Migration

Cell migration was studied by employing the "wound healing" assay. Briefly, cells were seeded in 24 wells dishes and cultured until confluence. Cells were treated with vehicle, lactate or 3,5 - DHBA and were then scraped with a 200 µl micropipette tip and monitored at 0, 24, and 48 h. The uncovered wound area was measured and quantified at different intervals with ImageJ 1.37v (NIH).

Immunoblotting

Briefly, for western blot analysis, 30 µg of protein was loaded onto a 12% polyacrylamide gel MiniPROTEAN® TGXTM (BIO-RAD, Milan, Italy) followed by electrotransfer to nitrocellulose membrane TransBlot® TurboTM (BIO-RAD, Milan, Italy) using TransBlot® SE Semi-Dry Transfer Cell (BIO- RAD, Milan, Italy). Subsequently, membrane was blocked in Odyssey Blocking Buffer (Licor, Milan, Italy) for 1 h at room temperature. After blocking, membrane was three times washed in phosphate-buffered saline (PBS) for 5 min and incubated with primary antibodies against MCT1 (1:1000), MCT4 (1:1000), β-catenin (1:500), E-Cadherin (1:500) and β-actin (1:1000) (anti-mouse, Cat. No. 4967S, Cell Signalling Technology, Milan, Italy), overnight at 4°C. Next day, membranes were washed three times in PBS for 5 min and

incubated with infrared anti-mouse IRDye800CW (1:5000) and anti-rabbit IRDye700CW secondary antibodies (1:5000) in PBS/0.5% Tween-20 for 1 h at room temperature. All antibodies were diluted in Odyssey Blocking Buffer. The blots were visualized using Odyssey Infrared Imaging Scanner (Licor, Milan, Italy), and protein levels were quantified by densitometric analysis. Data were normalized to β-actin expression.

Real-time RT-PCR for gene expression analysis

RNA was extracted by Trizol® reagent (Invitrogen, Carlsbad, CA, USA). First-strand cDNA was then synthesized with Applied Biosystem (Foster City, CA, USA) reverse transcription reagent. Quantitative real-time PCR was performed in Step One Fast Real-Time PCR System Applied Biosystems, using the SYBR Green PCR MasterMix (Life Technologies, Monza, Italy). The specific PCR products were detected by SYBR Green fluorescence. The relative mRNA expression level was calculated by the threshold cycle (Ct) value of each PCR product and normalized with that of actin by using a comparative $2 - \Delta\Delta Ct$ method. The sequence of primers used are presented in Table 1.

Table 1
List of qRT-PCR primers.

Gene of interest	Forward primer (5' ⟶ 3')	Reverse primer (5' ⟶ 3')
PGC1α	ATGAAGGGTACTTTTCTGCCCC	GGTCTTCACCAACCAGAGCA
SIRT1	AGGCCACGGATAGGTCCATA	GTGGAGGTATTGTTTCCGGC
TFAM	CCGAGGTGGTTTTCATCTGT	AGTCTTCAGCTTTTCCTGCG
ND4	CCAGTGGAATGCCTTGCCTA	TTGATCGCGGTGAGATTCCC
CyB	ACGAGCCACCGAAACAGAAT	ACGATTTTCGCCAGTCACCT
COX II	ACGACCTCGATGTTGGATCA	ATCATTTACGGGGGAAGGCG
COX IV	GCGGCAGAATGTTGGCTAC	AGACAGGTGCTTGACATGGG
ATP synthase	CCGCCTTCCGCGGTATAATC	ATGTACGCGGGCAATACCAT
MCT1	TGTTGTTGCAAATGGAGTGT	AAGTCGATAATTGATGCCCATGCCAA
MCT4	TATCCAGATCTACCTCACCAC	GGCCTGGCAAAGATGTCGATGA
HCAR1	TTCGTATTTGGTGGCAGGCA	TTTCGAGGGGTCCAGGTACA
β-Actin	CCTTTGCCGATCCGCCG	AACATGATCTGGGTCATCTTCTCGC

Zebrafish model

Adult zebrafish (Danio rerio) were housed in the Model Organism Facility – Center for Integrative Biology (CIBIO) University of Trento and maintained under standard conditions [16]. All zebrafish studies were

performed according to European and Italian law, D.Lgs. 26/2014, authorization 148/2018-PR to M. C. Mione. Fishes with somatic and germline expression of oncogenic HRAS were generated as described [17, 18].

The following zebrafish transgenic lines were used in the course of this study:

Et(zic4:Gal4TA4, UAS:mCherry) $_{hzm5}$ called zic:Gal4 [17]

Tg(UAS:eGFP-HRAS_G12V) $_{io006}$ called UAS:RAS [18]

The characterization of the GBM model is described in detail in Mayrhofer et al., 2017 [17].

Gene expression analysis

The analysis of expression of genes involved in glycolysis in zebrafish brain tumors was performed on previously generated data (GSE74754, https://www.ncbi.nlm.nih.gov/geo/query/acc.cgi?acc=GSE74754). The heatmap was generated using the web application heatmapper (http://www.heatmapper.ca/) .

For gene expression analysis of further samples, total RNA was extracted from larval heads and brains/tumors with TRIzol reagent (Invitrogen). Total RNA was cleaned up using RNeasy Mini Kit (Qiagen) following the manufacturer's instructions and treated twice with DNase I (1 unit/µg RNA, Qiagen). The RNA concentration was quantified using nanodrop2000 (Thermo Fisher) and VILO superscript KIT (Thermo Fisher) was used for First-strand cDNA synthesis according to the manufacturer's protocol. qRT-PCR analysis was performed using qPCR BIO Sygreen Mix (Resnova - PCR Biosystem) using a standard amplification protocol. The primers used for zebrafish mct1 were: forward 5'-GTCACCATTGTGGAATGTGC-3' and reverse 5'-TCATCATAGATATCGTTGAGTCGTC-3'; for hcar1 zebrafish were: forward 5'- CATCGTCATCTACTGCTCCAC-3' and reverse 5'- GCTAACACAAACCGCACA-3'; for zebrafish rps11 (housekeeping): forward: 5'-ACAGAAATGCCCCTTCACTG-3' and reverse: 5'-GCCTCTTCTCAAAACGGTTG-3'. Real-time PCR was performed with a CFX96 Real-Time PCR Detection System (Bio-Rad) machine. Q-PCR analysis was performed with Microsoft Excel and Graphpad Prism. In all cases, each PCR was performed with triplicate samples and repeated with at least two independent samples.

Immunofluorescence in zebrafish

Adult zebrafish resulting from crosses between zic:Gal4 and UAS:RAS, or from somatic expression of UAS:RAS [19], were screened under a fluorescent stereomicroscope for the presence of GFP-HRAS^{G12V} brain masses. Positive fish (over 90% of screened fish) were sacrificed by MS222 overdose, their brains removed, fixed and sectioned as previously described (Mayrhofer et al., 2020).

Sections were then washed in PBS (pH 7.4) and incubated primary antibodies diluted in PBS containing 5% normal goat serum and 0.1% triton x-100 at 4°C overnight. The antibody used and their dilutions were as follows: MCT1(abcam, 1:100) and HCAR1 (abcam, 1:100), Phospho Histone 3 (Abcam, 1:1000). A

secondary antibody conjugated with Alexa 546 (Abcam, 1:250) was used for 2 hour at room temperature, and nuclei were counterstained with DAPI. Images were acquired using an inverted Leica TSP8 confocal microscope. For whole-mount immunofluorescence of 5 day postfertilization (dpf) zebrafish, larvae of the zic: Gal4 line (controls) or zic:Gal4 x UAS:RAS line (tumor) were treated with 20 mM lattate or 10 mM AZ3965 in 1% DMSO in E3, or with 1% DMSO alone. Solutions with the drugs were changed every day starting at 1dpf till 5dpf, when the larvae were culled by anaestetic overdose, fixed in 4% PFA for 2 to 12 hrs at 4 C, their brains carefully removed under a stereomicoscope and processed with Ph3 antibody, diluted 1:1000 in 5% NGS, 0.5% Triton X100 in PBS overnight. A secondary antibody conjugated with Alexa 546 was used for 6 hour at room temperature. Images were acquired using an inverted Leica TSP8 confocal microscope, after equilibrating the brains in 100% glycerol.

Seahorse on zebrafish

For Seahorse analysis, tumors from adult fish or control brains were dissociated with a pipette tip in the assay medium provided by the manufactor, passed through a 40 mM sieve and counted. 50K cells were seeded on poly-L-Lysin coated Seahorse XFP plates and incubated for 20 min in the absence of CO2 before adding medium up to a final volume of 180 ul.

XF mitostress test kit including oligomycin, carbonyl cyanide p-trifluoromethoxy-phenylhydrazone (FCCP), and Rotenone A were obtained from Seahorse Bioscience Inc. (Billerica, MA, USA). XFp cell culture plates, sensor cartridges and XF base medium were also purchased from Seahorse Bioscience Inc. The Agilent Seahorse XFp Sensor Cartridge is hydrated in Agilent Seahorse XF Calibrant at 28°C in a non-CO2 incubator overnight. Control and tumor zebrafish brain cells are plated in the Agilent Seahorse XFp Cell Culture Miniplate at the desired density (50 K per well) using the appropriate cell culture growth medium. PBS 1X is added to the chambers to prevent evaporation of the culture medium. Within 1 hour from plating the Agilent Seahorse XFp Cell Culture Miniplate is put into a 28°C non-CO2 incubator for 1 hour prior to the assay.

Mito stress test assay

Assay medium is prepared by supplementing Agilent Seahorse XF Base Medium with 1 mM pyruvate, 2 mM glutamine, and 10 mM glucose bringing the pH to 7.4 with 0.1 N NaOH. Cells are placed in 28°C incubator with 5% CO2.

Injections of oligomycin, FCCP and Rotenone A were diluted in the assay medium following Agilent Seahorse XFp Mito Stress Test User Guide and loaded into ports A, B and C, respectively. The machine was calibrated, and the assay was performed using mito stress test assay protocol as suggested by the manufacturer (Seahorse Bioscience, Billerica, MA, USA). ECAR was measured under basal conditions followed by the sequential addition of oligomycin, FCCP and Rotenone A.

Data analysis

The XF reports of mito stress data were analysed with the freeware Wave and exported to Excel and Prism for further analysis and visualization.

Human gene expression

Dataset selection

The NCBI Gene Expression Omnibus (GEO) database (http://www.ncbi.nlm.nih.gov/geo/) [20] was used to select transcriptomes datasets of interest. Mesh terms “human”, “glioblastoma”, and “tumor grade”, were used to identify the datasets. We sorted the datasets by the number of samples (High to Low), age and sex of the participants and by the clinical data made available by the authors. We selected the GSE108474 dataset [21] over the others available for the number of subjects recruited (541), for the availability of clinical data (tumor staging) and for the variety of tumors analyzed (glioblastoma, oligodendrocytoma, astrocytoma and normal subjects).

Data processing, experimental design and statistics

To process and identify Significantly Different Expressed Genes (SDEG) within the datasets, we used the MultiExperiment Viewer (MeV) software (The Institute for Genomic Research (TIGR), J. Craig Venter Institute, La Jolla, USA). In cases where multiple genes probes have insisted on the same GeneID NCBI, we used those with the highest variance.

For GSE108474 (Table 2) we performed a statistical analysis with GEO2R, applying a Benjamini & Hochberg (False discovery rate) [22–24]. In Table 2 the sample detection from GSE dataset.

Table 2
Samples selected from GSE108474

Disease type	Number	Grade
NT	28	Negative
Astrocytoma	148	G2=65; G3=58; Na=25
Oligodendrocytoma	67	G2=30; G3=23; Na =14
Glioblastoma	221	G4=130; Na =91
G= tumor grade; Na= not assigned; NT= non tumor		

Significant differences between groups were assessed using the Ordinary one-way ANOVA test, and Tukey’s multiple comparisons test correction was performed to compare data between all groups. Correlations were determined using Pearson correlation. All tests were two-sided and significance was determined at adjusted p value 0.05. The dataset selected was transformed for the analysis in Z-score intensity signal. Z score is constructed by taking the ratio of weighted mean difference and combined standard deviation according to Box and Tiao (1992) [25]. The application of a classical method of data

normalization, z-score transformation, provides a way of standardizing data across a wide range of experiments and allows the comparison of microarray data independent of the original hybridization intensities. The z-score it is considered a reliable procedure for this type of analysis and can be considered a state-of-the-art method, as demonstrated by the numerous bibliography [26–37].

The efficiency of each biomarker across the different tumor grade was assessed by the receiver operating characteristic (ROC) curve analyses [38–40]. The ROC curves analyzed brain biopsies of healthy subjects (NT) vs glioblastoma patients, astrocytoma vs glioblastoma, and oligodendroglioma vs glioblastoma. The area under the ROC curve (AUC) and its 95% confidence interval (95% CI) indicates diagnostic efficiency. The accuracy of the test with the percent error is reported [41].

Results

We first analysed the effects of lactate on 3 human GBM cell lines (i.e. U-87 MG, A-172 and U-251 MG) by performing a clonogenic assay on lactate exposed cells (figure S1). We observed that lactate induced an increase of about 2-fold of both number (78.3 ± 9.0 control versus 151.0 ± 17.1 lactate) and area (123.2 ± 8.2 control versus 215.0 ± 30.4 lactate) of colonies of U-87 MG cells (figure S1). Interestingly, analysis of clonogenicity on A-172 revealed that lactate reduced the total number of colonies (35.7 ± 0.3 control versus 21.0 ± 1.2 lactate, figure S1), but dramatically affected the area of colonies that was more than 4-fold increased as compared to control cultures (731.3 ± 0.5 control versus 3470.8 ± 30.3 lactate, figure S1). We also repeated our analysis on U-251 MG cell, that showed similar response to lactate as U-251 MG cells, with a significant increase of the total number of colonies (26.5 ± 0.9 control versus 38.0 ± 3.6 lactate) and mean colony area (700.0 ± 7.1 control versus 1409.4 ± 28.0 lactate, figure S1).

We then moved to compare the effect of increased levels of extracellular lactate with the selective stimulation of the lactate receptor hydroxycarboxylic acid receptor 1 (HCAR1) mediated by 3,5-dihydroxybenzoic acid (3,5-DHBA). We observed in all tested cells a significant increase of normalized cell index after lactate exposure (figure 1a-c), confirmed by an increase of the total area under the curve for U-87 MG (76.5 ± 0.4 lactate versus 38.9 ± 0.2 control, figure 1a), A-172 (86.6 ± 0.8 lactate versus 64.4 ± 0.4 control, figure 1b) and U-251 MG (78.1 ± 1.1 lactate versus 40.5 ± 0.8 control, figure 1c). 3,5-DHBA stimulation was also able to induce similar effects on cell proliferation on U-87 MG, A-172 and U-251 MG cell line, showing increased normalized cell index in all tested cell lines (figure 1a-c), confirmed by an increase of the total area under the curve for U-87 MG (106.3 ± 2.4, figure 1a), A-172 (134.6 ± 1.1, figure 1b) and U-251 MG (122.9 ± 1.3, figure 1c). We then tested whether lactate affects cell migration of GBM cells. Interestingly, we observed a reduced % of wideness of scratch assay test at 24 and 48 hours in all tested cells lines (figure 1d-g). We also confirmed the effects of HCAR stimulation through 3,5-DHBA on cell migration, finding a significantly reduced % of wideness of scratch assay test at 48 hours in all tested cells lines (figure 1d-g).

In an effort to link lactate, as a positive modulator of cell proliferation and migration, to the underlying molecular mechanisms activated in GBM cell lines, we performed western blot analysis for lactate

transporters MCT1 and MCT4, and for β-Catenin and E-Cadherin on control and lactate treated U-87 MG, A-172 and U-251 MG cells.

We found that U-87 MG cells responds to increased levels of extracellular lactate by increasing the levels of MCT1 transporter of about 2.5-fold as compared to control cultures and slightly, but significantly, reducing MCT4 expression levels (figure 2a).

Importantly, the β-Catenin protein levels were found to be significantly increase of about 6-fold in lactate exposed U-87 MG cells and such a modulation was coupled with reduced expression levels of E-Cadherin (figure 2a).

Notably, analysis of A-172 and U-251 MG exposed to increased extracellular lactate levels, revealed some differences in cellular responses as compared to U-87 MG cells. Indeed, we confirmed that exposure to lactate increased MCT1 and β-Catenin expression levels in both A-172 (figure 2b) and U-251 MG (figure 2c) but showed that both cell lines respond to lactate also inducing significantly higher MCT4, increased of about 1.2-fold in both cell lines, and E-Cadherin expression levels (figure 2b-c).

Given the evidence on cellular modulation exerted by increased extracellular levels of lactate, we sought to link molecular mechanisms underlying these phenomena with the activation of lactate receptor HCAR1. We first investigated HCAR1 mRNA expression levels on U-87 MG, A-172 and U-251 MG cell lines after exposure to lactate, finding a significant increase of HCAR1 mRNA levels in all tested cells at 24 hours (figure 2d). We then moved to evaluate the effects of 3,5-DHBA, confirming a significant increase of HCAR1 mRNA levels at 24 hrs post 3,5-DHBA incubation in all tested cell lines (figure 2e).

To find whether HCAR1 selective stimulation was able to increase lactate transporters MCT1 and MCT4 we also checked the mRNA expression levels of these transporters, finding that 3,5-DHBA stimulation was able to significantly increase MCT1 expression of about 25-fold, 5-fold and 13-fold in U-87 MG, A-172 and U-251 MG, respectively (figure 2f). Such evidences were coupled with contrasting data on the other tested transporter MCT4. Indeed, we observed that U-87 MG cells respond to 3,5-DHBA stimulation by increasing MCT4 mRNA expression of about 2-fold (figure 2g), but A-172 showed no significant changes in MCT4 expression and U-251 MG cells showed a significant reduction of MCT4 expression upon treatment with 3,5-DHBA as compared to untreated cells (figure 2g).

To further expand our evidences on molecular mechanisms induced by the increase of extracellular lactate, we analyzed a panel of mRNAs of genes involved in mitochondrial activity and energy metabolism. Our data show that U-87 MG significantly increase of about 4-fold the relative mRNA levels of transcription factor A mitochondrial (TFAM), PPARG coactivator 1 alpha (PGC1a) and sirtuin 1 (SIRT1) (figure 3a-b), coupled with an overall increase of ATP synthase (ATP syn), cytochrome c oxidase subunit 4 (COX IV) and COX II, mitochondrial Cytochrome b (CYTB) and mitochondrial NADH-ubiquinone oxidoreductase chain 4 (ND4, figure 3a), when exposed to lactate for 24 or 48 hours as compared with untreated cells (figure 3a-b). These observations were confirmed in A-172 (figure 3c-d) and U-251 MG cell lines (figure 3e-f). Specifically, we observed superimposable effects on A-172 as compared to U-87 MG

cells, where U-251 MG showed an increase of about 15-fold of TFAM, PGC1a and SIRT1 at 48 hours as compared to untreated cells (figure 3f), coupled with a slight reduction of COX IV mRNA at the same timepoint (-1.87 ± 0.1 $\log_2$ fold change over control, figure 3e). We also performed a computer-assisted analysis of mitotracker fluorescence intensity on control versus lactate treated cells, finding that lactate was able to significantly increase cytoplasmic mitotracker intensity 18 hrs post treatment (figure 3g-h).

To link intracellular mediators of mitochondrial fitness with HCAR stimulation, we performed an mRNA expression level analysis of PGC1a, TFAM, SIRT1, ATP syn, COX II and COX IV on 3,5-DHBA stimulated cells. Our analysis revealed that U-87 MG cells exposed to 3,5-DHBA recapitulate the molecular mRNA activation observed with lactate (figure 4a-b). Indeed, all tested genes, except for TFAM, were significantly increased in cultures exposed to HCAR stimulation (figure 4b). These data were confirmed in A-172 cells that showed increased levels of all tested genes upon 3,5-DHBA stimulation (figure 4c-d). Finally, U-251 MG showed a very similar mRNA expression profiles, but we observed that HCAR stimulation through 3,5-DHBA did not modulate PGC1a expression at tested timepoint on this cell line (figure 4e-f).

To finally link HCAR stimulation with the effects on mitochondria observed on GBM cell lines exposed to increased extracellular lactate levels, we performed a mitotracker analysis, finding a significant increase of normalized intensity in 3,5-DHBA stimulated cells as compared to control cultures (figure 4g).

Given the capability of extracellular lactate to modulate β-Catenin and E-Cadherin expression levels, we performed a western blot analysis on 3,5-DHBA stimulated A-172 cells. Our analysis revealed that HCAR1 activation induces a significant increase of β-Catenin protein expression levels as compared to control cultures and this phenomenon was coupled with a significant reduction of E-Cadherin (figure 4h), revealing that lactate may also act via additional mechanisms that induce E-Cadherin not related to HCAR1 activation.

To investigate whether lactate accumulation, resulting from increased glycolysis, may have similar effects *in vivo*, we used a zebrafish model of glioblastoma [17] (figure 5a), and analysed the metabolic phenotype of these tumors. Comparison of the expression levels of 29 genes encoding for enzymes and transporters involved in the glycolytic pathway acquired through RNA-Seq (GSE74754, https://www.ncbi.nlm.nih.gov/geo/query/acc.cgi?acc=GSE74754), revealed increased expression (log2 FC >1.2, P-value <0.001 or adjusted P-value <0.05) of 26 out of 29 genes, with *aldh1a3, hk2 and hcar1-3* being the most upregulated in tumors (figure 5b). We then performed a mitostress test on freshly dissociated zebrafish control and tumor brains using the Seahorse XFp apparatus. This test confirmed that upon blockage of energy production through mitochondrial respiration, zebrafish GBM cells experience a huge increase of the extracellular acidification rate (ECAR), indicating a prominent role of anaerobic glycolysis in energy production, accompanied by increased proton leak (leading to high ROS production) and lower ATP yield (figure 5c). Staining for MCT1 and HCAR1 in sections of zebrafish brain tumors revealed an increase in the number of both MCT1+ and HCAR1+ cells (figure 5d), whereas q-PCR analysis of mRNA expression for *mct1* and *hcar1* revealed a significant increase in expression for *mct1* in

adult tumors compared to control brain, and a significant increase in expression of *hcar1* in both adult brain tumors and in 5days post-fertilization (dpf) larvae expressing oncogenic RAS (figure 5e).

Then, we evaluated the effects of exposing to lactate or to the MCT1 inhibitor, AZ3965 (AZD), on the proliferation rate of control brains and brains expressing oncogenic RAS, using immunostaining for a mitotic marker (phospho-serine 10 on histone 3, PH3). Incubation of developing larvae from 1 to 5 dpf with 20 uM lactate induced a significant increase in proliferation in brains expressing oncogenic RAS, but not in control brains, while treatment with 10 uM AZD did not affect the proliferation rate in either control or RAS expressing brains (figure 5f**).**

MCT1 gene expression analysis as a diagnostic and prognostic marker of glioma

The MCT1 gene expression analysis obtained from the GSE108474 dataset showed that there were significant differences when the expression levels obtained from brain biopsies of glioblastoma patients were compared to the other brain tumors stages. (figure 6). Specifically, patients with glioblastoma expressed significantly higher levels of the MCT1 messenger in the brain than patients with oligodendrocytoma ($p<0.0001$), astrocytoma ($p<0.0001$), or healthy subjects ($p<0.0001$) (figure 6a). This finding was confirmed by the significantly positive correlation between MCT1 expression levels and tumor grade ($r = 0.4026$; $p = 0.0223$) (figure 6b). According to these results, we investigated the prognostic potential of MCT1 expression in the progression of main brain tumors. Currently the expression analysis of Isocitrate Dehydrogenase (NADP (+)) 1 (IDH1) and the identification of its main mutations (e.g. R132H) are used for glioma diagnosis and prognosis [42]. By carrying out a Pearson correlation analysis between MCT1 and IDH1 brain tumor expression levels, we highlighted that in glioblastoma patients the expression levels of the two genes were significantly closely inversely correlated ($r = -0.4163$, $p <0.0001$) (figure 6c). Furthermore, in order to evaluate the potential diagnostic ability of MCT1 gene expression to discriminate against the brain tumors stages, we performed a Receiver operating characteristic (ROC) analysis. We confirmed the diagnostic ability of MCT1 to discriminate the glioblastoma patients from healthy subjects (AUC=0.7558, $p<0.0001$) (figure 6d) or from the patients affected to astrocytoma (AUC=0.7775, $p<0.0001$) (figure 6e) or oligodendrocitoma (AUC=0.8104, $p<0.0001$) (figure 6f).

Discussion

Cell metabolism and its related intercellular signalling has been shown to be of great importance in a number of physiological and pathological processes [43]. In the present study, we first evaluated the effects of lactate on three human GBM cell lines, finding that it increases both migration and cell proliferation. Such a phenomenon was linked to a potential lactate dependent HCAR1 activation, as observed using 3,5-DHBA, a selective HCAR1 agonist.

Several authors showed that stimulation of HCAR1 leads to the activation of cell survival signalling promoting cell proliferation via the inhibition of apoptosis and stimulates the secretion of several angiogenic factors in a PI3K/Akt-CREB signalling pathway-dependent manner [44]. Interestingly, an

essential part of the repair process after a neonatal brain injury is the generation of new cells by increase of proliferation and differentiation of stem cells, Lauritz H. K. et al., by neurosphere assays, demonstrated that the cells lacking HCAR1 had reduced proliferation ability [45].

Moreover, MCT1 is mainly used by oxidative cells to intake extracellular lactate and MCT4 is mainly used to release accumulated lactate into the extracellular milieu, in many cases by hypoxic and/or highly glycolytic cells [46–48]. Our data support the hypothesis that lactate leads GBM cells to increase HCAR1, acting as a sensor, levels and MCT1, mediating lactate intake from the extracellular milieu. This phenomenon is coupled with increased mitochondrial content and fitness, thus prompting GBM cells towards oxidative metabolism. It is worth noticing that this mechanism is not related to the increased lactate level itself but is dependent on the agonism on HCAR1 receptor. Indeed, we were able to reproduce these metabolic reshaping using the selective HCAR1 agonist 3,5-dhba. Consistently, a study performed in GPR81-silenced pancreatic cancer cells led to reduced mitochondrial activity and survival in several cancer cell [49]. In particular, several cancer cell types, including colon, breast, lung, cervical, and pancreatic showed an increase of HCAR1 expression and functional studies indicated that it is important for lactate regulation of genes involved in lactate uptake and metabolism. Moreover, HCAR1 is critical for cancer cell survival only when glucose was absent and in the presence of lactate [50].

Interestingly, we observed critical differences in cell response to HCAR1 activation analyzing MCT4 levels. Indeed, we observed that 24 hrs of exposure to lactate mediated a reduction of MCT4 protein levels in U-87 MG, whether we found a significant MCT4 increase in both U-251 MG and A-172. Such differential response to lactate among tested cell lines, may be linked to the metabolic reshaping of these cells. Noteworthy, quantification of the main mitochondrial genes revealed that U-87 MG cells underwent a rapid increase of mitochondrial content, although less pronounced versus basal levels, as compared to that of A-172 and U-251 MG. Our data suggest that U-87 MG have a different response as compared to the other cell lines in terms of timing to repurpose their transporters and metabolism. Indeed, upon 3,5-DHBA stimulation of HCAR1 we observed a significant increase of MCT4 in U-87 MG, where we obtained contrasting results for A-172 and U-251 MG.

This set of experiments suggest that HCAR1 activation induces MCT1 increase, thus mediating lactate intake in stimulated cells. It is therefore conceivable that intercellular metabolism and mitochondrial content are closely related to HCAR1 activation by several pathways including lactate as a metabolite and other receptor-mediated mechanisms. To this regard, Zaho Y., et al., showed that increasing lactate concentration in liver tumor microenvironment could activate HCAR1 receptor and facilitate MCT1-mediated uptake of lactate, leading to increased ATP production and decrease of the AMP:ATP ratio in the intracellular compartment [51]. Tumor cells stimulate mitochondrial biogenesis not only for proliferation but also for promoting malignant transformation, in migration and invasiveness and during tumor adaptation to hypoxia [52, 53]. As previously mentioned, we observed an increase of mitochondrial biogenesis in GBM cell treated with lactate or HCAR1 inducer, this phenomenon could be due to the increase of lactate uptake after MCT1 overproduction. Moreover, we also showed that the increase of mitochondrial mass also induces an increase of OXPHOS gene expression. Exogenous treatment of

lactate in various tumor cell lines induced an increase in ROS levels. We hypothesize that this latter increase in oxidative state determines an enhances of mitochondrial biogenesis such as showed by increase of PGC1a, SIRT1 expression and oxidative genes.

Interestingly, our results indicate also that HCAR1 activation promotes the modulation of b-catenin and e-cadherin expression suggesting that lactate participates to the epithelial-mesenchymal transition (EMT) in GBM. Several studies have been conducted investigating the metabolic changes during EMT in breast, lung, and ovarian cancers, following an increased recognition of metabolic reprogramming as a hallmark of tumor development [54–56].

Lactate produced and exported by tumor cells can be also used by adjacent tumor cells, in the tumor microenvironment, including endothelial cells and stromal cancer-associated fibroblasts, reprogramming their functions, and contributing to tumor progression [57]. Consequently, several authors hypothesized that lactate might also modulate the same epigenetic mechanisms in adjacent normal cells modulating also EMT processes [58, 59].

Given the insights coming from in vitro experiment on relevant human GBM cell lines, we enrolled a HRAS overexpressing zebrafish model of GBM to test whether similar metabolic changes are taking place in this model. Our data confirmed a widespread upregulation of glycolytic enzymes, with upregulation of HCAR1, thus indicating a prominent role for lactate signalling. In the tumor microenvironment HCAR1 upregulation was coupled with a significantly increased proton leak and less efficient ATP production. The increased expression of lactate transporters (*mct1*) and sensor (*hcar1*) was already present at 5 dpf, when tumors start to grow.

Lactate exposure determined a significant increase in proliferating PH3 positive cells in RAS-overexpressing zebrafish brain, but not in control brains, and this was reverted by selective inhibition of MCT1. This evidence suggests that lactate intake support cell proliferation in cancer and that metabolic reshaping is a critical stimulus in GBM microenvironment. Thus, both cell culture and in vivo studies, using different approaches and different genes, converge toward the same conclusion, i.e. that glycolysis is prominent in GBM and leads to massive lactate production which shapes the microenvironment towards an aggressive phenotype and represent a valid therapeutic target.

Our data from human GBM biopsies were also consistent with preclinical evidence we are providing herein. We observed that in high proliferative GBM biopsies, KI67 negative cells were expressing significantly higher levels of MCT1 as compare to proliferative cells and low proliferative GBM cells. This indicates that GBM cells response to lactate, besides sustaining metabolic reshaping and response, it favours proliferation of neighbourhood cells by cooperating with their glycolytic metabolism, sensing and removing extracellular lactate. Our data is consistent with other studies in patients with advanced cancer showing that MCT-1 inhibition may provide a significant role in cancer growth and progression and may represent a druggable target for development of new therapeutic strategies (ClinicalTrials.gov identifier (NCT number): NCT01791595).

Further confirmation of our study was obtained by analyzing the human GSE108474 dataset. The analysis allowed us to highlight that MCT1 is significantly modulated during the progression of the disease. In particular, significant expression changes were highlighted with the increase in the degree of malignancy. Furthermore, our results showed that MCT1 can potentially be used in order to discriminate patients with glioblastoma versus those with astrocytoma and oligodendrocytoma. These data are in agreement with the current bibliography which considers MCT1 a new prognostic biomarker and potentially target in human glioblastoma [60]. Interestingly, the correlation analysis between MCT1 and IDH1 brain expression levels in glioblastoma patients was inversely proportional, further confirming recently obtained data in which mutant IDH1 expression is associated with down-regulation of monocarboxylate transporters [61].

Conclusion

In conclusion, we showed that lactate is involved in various mechanisms favoring tumor development and progression. In particular, lactate possesses a dual role being involved in the metabolic changes of tumor cells and acting as a molecule promoting cellular signaling through its membrane receptors. The ability to metabolically shift from glycolytic to oxidative metabolism and vice versa, is likely to confer an advantage in survival, progression and drug resistance. A glycolytic metabolism (Warburg effect) certainly in the first phase of disease expansion, determines an advantage in tumor proliferation. The lactate thus produced in the tumor microenvironment favors, on the one hand, the immune escape mechanisms, on the other, it may modify the metabolism of the adjacent tumor cells, becoming more oxidative and therefore more resistant also to antiblastic therapies. Therefore, lactate metabolism may be considered as a therapeutic target to develop novel pharmacological strategies to GBM therapy and improve the outcome and quality of life of such patients.

List Of Abbreviations

3,5-DHBA 3,5-Dihydroxybenzoic acid

Akt Protein kinase B

ATP syn ATP synthase

AUC Area under curve

COX II Cytochrome c oxidase subunit 2

COX IV Cytochrome c oxidase subunit 4

CREB cAMP response element-binding protein

CyB Mitochondrial Cytochrome b

dpf Day postfertilization

EMT Epithelial mesenchymal transition

FBS Fetal bovine serum

FCCP Carbonyl cyanide p-trifluoromethoxy-phenylhydrazone

GBM Glioblastoma multiforme

GEO Gene Expression Omnibus

GPR81 G protein-coupled receptor 81

HCAR1 Hydroxycarboxylic acid receptor 1

HCS High content screening

HPI High proliferative index

IDH1 Isocitrate Dehydrogenase 1

LPI Low proliferative index

MCTs Monocarboxylate transporters

ND4 Mitochondrial NADH-ubiquinone oxidoreductase chain 4

OXPHOS Oxidative phosphorilatin

PGC1α PPARG coactivator 1 alpha

PH3 Phospho Histone 3

PI3K PhosphatidylInositol 3-Kinase

ROC Receiver operating characteristic

ROS Reactive oxygen species

RTCA Real-Time Cell Analyser

SIRT1 Sirtuin 1

TFAM Transcription factor A mitochondrial

TME Tumor microenvironment

WHO World Health Organization

Declarations

Ethics approval

Not applicable.

Consent for publication

Not applicable.

Availability of data and materials

The datasets used and/or analysed during the current study are available from the corresponding author on reasonable request.

Competing interests

The authors declare that they have no competing interests

Funding

LL was supported by the international Ph.D. program in Neuroscience (Department of Biomedical and Biotechnological Sciences, University of Catania, Italy). This study was supported by Piano di Incentivi per la ricerca di Ateneo 2020/2022 Linea di intervento 2 (G.L.V.). NV was supported by the PON AIM R&I 2014-2020-E66C18001240007, C.G. was supported by the PON AIM R&I 2014–2020-E68D19001340001.

Authors' contributions

Conceptualization: NV, DT, GMVB, AG, MCM, GLV; Project administration: LL, NV, DT, CG, AG, MCM, GLV; Methodology: LL, NV, DT, GB, MB, MDR, RP, MCM, GLV; Investigation: LL, NV, DT, CG, GB, MB, MDR; Formal analysis: LL, NV, DT, RC, GMVB, MDR, RP, AG, MCM, GLV; Resources: DT, RC, RP, MCM, GLV; Supervision: LL, NV, DT, RP, AG, MCM, GLV; Writing-Original Draft: LL, NV, DT, MCM, GLV; Writing-Reviewing and Editing: LL, NV, DT, CG, GMVB, MDR, RP, AG, MCM, GLV.

Acknowledgements

The authors acknowledge the confocal microscopy facility at the Bio-Nanotech Research and Innovation Tower (BRIT) of the University of Catania (Italy).

References

1. Stupp R, Hegi ME, Mason WP, van den Bent MJ, Taphoorn MJ, Janzer RC, et al. Effects of radiotherapy with concomitant and adjuvant temozolomide versus radiotherapy alone on survival in

glioblastoma in a randomised phase III study: 5-year analysis of the EORTC-NCIC trial. Lancet Oncol. 2009;

2. Torrisi F, Vicario N, Spitale FM, Cammarata FP, Minafra L, Salvatorelli L, et al. The role of hypoxia and src tyrosine kinase in glioblastoma invasiveness and radioresistance. Cancers (Basel). 2020.
3. Charles N, Holland EC. The perivascular niche microenvironment in brain tumor progression. Cell Cycle. 2010.
4. Liberti M V., Locasale JW. The Warburg Effect: How Does it Benefit Cancer Cells? Trends Biochem. Sci. 2016.
5. Heiden MGV, Cantley LC, Thompson CB. Understanding the warburg effect: The metabolic requirements of cell proliferation. Science (80-.). 2009.
6. Miranda-Gonçalves V, Bezerra F, Costa-Almeida R, Freitas-Cunha M, Soares R, Martinho O, et al. Monocarboxylate transporter 1 is a key player in glioma-endothelial cell crosstalk. Mol Carcinog. 2017;56.
7. Kobayashi M, Narumi K, Furugen A, Iseki K. Transport function, regulation, and biology of human monocarboxylate transporter 1 (hMCT1) and 4 (hMCT4). Pharmacol. Ther. 2021.
8. Park SJ, Smith CP, Wilbur RR, Cain CP, Kallu SR, Valasapalli S, et al. An overview of MCT1 and MCT4 in GBM: small molecule transporters with large implications. Am J Cancer Res. 2018;8.
9. Payen VL, Hsu MY, Rädecke KS, Wyart E, Vazeille T, Bouzin C, et al. Monocarboxylate transporter MCT1 promotes tumor metastasis independently of its activity as a lactate transporter. Cancer Res. 2017;77.
10. Garnier D, Renoult O, Alves-Guerra MC, Paris F, Pecqueur C. Glioblastoma stem-like cells, Metabolic strategy to kill a challenging target. Front. Oncol. 2019.
11. Hoque R, Farooq A, Ghani A, Gorelick F, Mehal WZ. Lactate reduces liver and pancreatic injury in toll-like receptor- and inflammasome-mediated inflammation via gpr81-mediated suppression of innate immunity. Gastroenterology. 2014;146.
12. Brown TP, Ganapathy V. Lactate/GPR81 signaling and proton motive force in cancer: Role in angiogenesis, immune escape, nutrition, and Warburg phenomenon. Pharmacol. Ther. 2020.
13. Ristic B, Bhutia YD, Ganapathy V. Cell-surface G-protein-coupled receptors for tumor-associated metabolites: A direct link to mitochondrial dysfunction in cancer. Biochim. Biophys. Acta - Rev. Cancer. 2017.
14. Ahmed K, Tunaru S, Tang C, Müller M, Gille A, Sassmann A, et al. An Autocrine Lactate Loop Mediates Insulin-Dependent Inhibition of Lipolysis through GPR81. Cell Metab. 2010;11.
15. Roland CL, Arumugam T, Deng D, Liu SH, Philip B, Gomez S, et al. Cell surface lactate receptor GPR81 is crucial for cancer cell survival. Cancer Res. 2014;74.
16. Detrich HW, Westerfield M, Zon LI. Essential zebrafish methods : cell and developmental biology. Reliab. lab Solut. 2009.

17. Mayrhofer M, Gourain V, Reischl M, Affaticati P, Jenett A, Joly JS, et al. A novel brain tumour model in zebrafish reveals the role of YAP activation in MAPK- and PI3K-induced malignant growth. DMM Dis Model Mech. 2017;10.
18. Santoriello C, Gennaro E, Anelli V, Distel M, Kelly A, Köster RW, et al. Kita driven expression of oncogenic HRAS leads to early onset and highly penetrant melanoma in zebrafish. PLoS One. 2010;5.
19. Idilli AI, Pagani F, Kerschbamer E, Berardinelli F, Bernabé M, Cayuela ML, et al. Changes in the expression of pre-replicative complex genes in hTERT and ALT pediatric brain tumors. Cancers (Basel). 2020;12.
20. Clough E, Barrett T. The Gene Expression Omnibus database. Methods Mol Biol. 2016.
21. Gusev Y, Bhuvaneshwar K, Song L, Zenklusen JC, Fine H, Madhavan S. Data descriptor: The REMBRANDT study, a large collection of genomic data from brain cancer patients. Sci Data. 2018;5.
22. Xiao J, Cao H, Chen J. False discovery rate control incorporating phylogenetic tree increases detection power in microbiome-wide multiple testing. Bioinformatics. 2017;33.
23. Smyth GK. Linear models and empirical bayes methods for assessing differential expression in microarray experiments. Stat Appl Genet Mol Biol. 2004;3.
24. Sean D, Meltzer PS. GEOquery: A bridge between the Gene Expression Omnibus (GEO) and BioConductor. Bioinformatics. 2007;23.
25. Box GEP, Tiao GC. Nature of Bayesian Inference. Bayesian Inference Stat Anal. 2011.
26. Cheadle C, Vawter MP, Freed WJ, Becker KG. Analysis of microarray data using Z score transformation. J Mol Diagnostics. 2003;5.
27. Scarpino M, Pinzone MR, Di Rosa M, Madeddu G, Focà E, Martellotta F, et al. Kidney disease in HIV-infected patients. Eur Rev Med Pharmacol Sci. 2013;17.
28. Feng C, Wu J, Yang F, Qiu M, Hu S, Guo S, et al. Expression of Bcl-2 is a favorable prognostic biomarker in lung squamous cell carcinoma. Oncol Lett. 2018;15.
29. Kang C, Huo Y, Xin L, Tian B, Yu B. Feature selection and tumor classification for microarray data using relaxed Lasso and generalized multi-class support vector machine. J Theor Biol. 2019;463.
30. Care MA, Barrans S, Worrillow L, Jack A, Westhead DR, Tooze RM. A Microarray Platform-Independent Classification Tool for Cell of Origin Class Allows Comparative Analysis of Gene Expression in Diffuse Large B-cell Lymphoma. PLoS One. 2013;8.
31. Wang J, Coombes KR, Highsmith WE, Keating MJ, Abruzzo L V. Differences in gene expression between B-cell chronic lymphocytic leukemia and normal B cells: A meta-analysis of three microarray studies. Bioinformatics. 2004;20.
32. Reddy TBK, Riley R, Wymore F, Montgomery P, Decaprio D, Engels R, et al. TB database: An integrated platform for tuberculosis research. Nucleic Acids Res. 2009;37.
33. Lê Cao KA, Rohart F, McHugh L, Korn O, Wells CA. YuGene: A simple approach to scale gene expression data derived from different platforms for integrated analyses. Genomics. 2014;103.

34. Chen QR, Song YK, Wei JS, Bilke S, Asgharzadeh S, Seeger RC, et al. An integrated cross-platform prognosis study on neuroblastoma patients. Genomics. 2008;92.
35. Mehmood R, El-Ashram S, Bie R, Dawood H, Kos A. Clustering by fast search & merge of local density peaks for gene expression microarray data. Sci Rep. 2017;7.
36. Yasrebi H, Sperisen P, Praz V, Bucher P. Can survival prediction be improved by merging gene expression data sets? PLoS One. 2009;4.
37. Cheadle C, Cho-Chung YS, Becker KG, Vawter MP. Application of z-score transformation to Affymetrix data. Appl Bioinformatics. 2003;2.
38. Lusted LB. Signal detectability and medical decision-making. Science (80-). 1971;171.
39. Castrogiovanni P, Sanfilippo C, Imbesi R, Maugeri G, Lo Furno D, Tibullo D, et al. Brain CHID1 Expression Correlates with NRGN and CALB1 in Healthy Subjects and AD Patients. Cells. 2021;10.
40. Catrogiovanni P, Musumeci G, Giunta S, Imbesi R, Di Rosa M. The expression levels of CHI3L1 and IL15Rα correlate with TGM2 in duodenum biopsies of patients with celiac disease. Inflamm Res. 2020;69.
41. Zetterberg H, Bozzetta E, Favole A, Corona C, Cavarretta MC, Ingravalle F, et al. Neurofilaments in blood is a new promising preclinical biomarker for the screening of natural scrapie in sheep. PLoS One. 2019;14.
42. Han S, Liu Y, Cai SJ, Qian M, Ding J, Larion M, et al. IDH mutation in glioma: molecular mechanisms and potential therapeutic targets. Br. J. Cancer. 2020.
43. Neagu M, Constantin C, Popescu ID, Zipeto D, Tzanakakis G, Nikitovic D, et al. Inflammation and metabolism in cancer cell—mitochondria key player. Front Oncol. 2019;9.
44. Lee YJ, Shin KJ, Park SA, Park KS, Park S, Heo K, et al. G-protein-coupled receptor 81 promotes a malignant phenotype in breast cancer through angiogenic factor secretion. Oncotarget. 2016;7.
45. Kennedy LH, Emilie R. Glesaaen, Vuk Palibrk, Marco Pannone, Wei Wang, Ali H.J. Al-Jabri, Rajikala Suganthan, Niklas Meyer, Xiaolin Lin, Linda H. Bergersen, View ORCID ProfileMagnar Bjørås VOPER. Lactate receptor HCAR1 regulates neurogenesis and microglia activation after neonatal hypoxia-ischemia. bioRxiv. 2020;
46. Kennedy KM, Dewhirst MW. Tumor metabolism of lactate: The influence and therapeutic potential for MCT and CD147 regulation. Futur. Oncol. 2010.
47. Sun X, Wang M, Wang M, Yao L, Li X, Dong H, et al. Role of Proton-Coupled Monocarboxylate Transporters in Cancer: From Metabolic Crosstalk to Therapeutic Potential. Front. Cell Dev. Biol. 2020.
48. Merezhinskaya N, Fishbein WN. Monocarboxylate transporters: Past, present, and future. Histol. Histopathol. 2009.
49. Hanahan D, Weinberg RA. Hallmarks of cancer: The next generation. Cell. 2011.
50. Wagner W, Kania KD, Blauz A, Ciszewski WM. The lactate receptor (HCAR1/GPR81) contributes to doxorubicin chemoresistance via abcb1 transporter up-regulation in human cervical cancer hela

cells. J Physiol Pharmacol. 2017;68.

51. Zhao Y, Li M, Yao X, Fei Y, Lin Z, Li Z, et al. HCAR1/MCT1 Regulates Tumor Ferroptosis through the Lactate-Mediated AMPK-SCD1 Activity and Its Therapeutic Implications. Cell Rep. 2020;33.
52. Cormio A, Guerra F, Cormio G, Pesce V, Fracasso F, Loizzi V, et al. Mitochondrial DNA content and mass increase in progression from normal to hyperplastic to cancer endometrium. BMC Res Notes. 2012;5.
53. Lebleu VS, O'Connell JT, Gonzalez Herrera KN, Wikman H, Pantel K, Haigis MC, et al. PGC-1α mediates mitochondrial biogenesis and oxidative phosphorylation in cancer cells to promote metastasis. Nat Cell Biol. 2014;16.
54. Li W, Wei Z, Liu Y, Li H, Ren R, Tang Y. Increased 18F-FDG uptake and expression of Glut1 in the EMT transformed breast cancer cells induced by TGF-β. Neoplasma. 2010;57.
55. Li J, Dong L, Wei D, Wang X, Zhang S, Li H. Fatty acid synthase mediates the epithelial-mesenchymal transition of breast cancer cells. Int J Biol Sci. 2014;10.
56. Jiang L, Xiao L, Sugiura H, Huang X, Ali A, Kuro-O M, et al. Metabolic reprogramming during TGFβ1-induced epithelial-to-mesenchymal transition. Oncogene. 2015;34.
57. Rattigan YI, Patel BB, Ackerstaff E, Sukenick G, Koutcher JA, Glod JW, et al. Lactate is a mediator of metabolic cooperation between stromal carcinoma associated fibroblasts and glycolytic tumor cells in the tumor microenvironment. Exp Cell Res. 2012;318.
58. Hanieh H, Ahmed EA, Vishnubalaji R, Alajez NM. SOX4: Epigenetic regulation and role in tumorigenesis. Semin. Cancer Biol. 2020.
59. Bhagat TD, Von Ahgrens D, Dawlaty M, Zou Y, Baddour J, Achreja A, et al. Lactate-mediated epigenetic reprogramming regulates formation of human pancreatic cancer-associated fibroblasts. Elife. 2019;8.
60. Miranda-Gonçalves V, Gonçalves CS, Granja S, de Castro JV, Reis RM, Costa BM, et al. MCT1 is a new prognostic biomarker and its therapeutic inhibition boosts response to temozolomide in human glioblastoma. Cancers (Basel). 2021;13.
61. Viswanath P, Najac C, Izquierdo-Garcia JL, Pankov A, Hong C, Eriksson P, et al. Mutant IDH1 expression is associated with down-regulation of monocarboxylate transporters. Oncotarget. 2016;7.

Figures

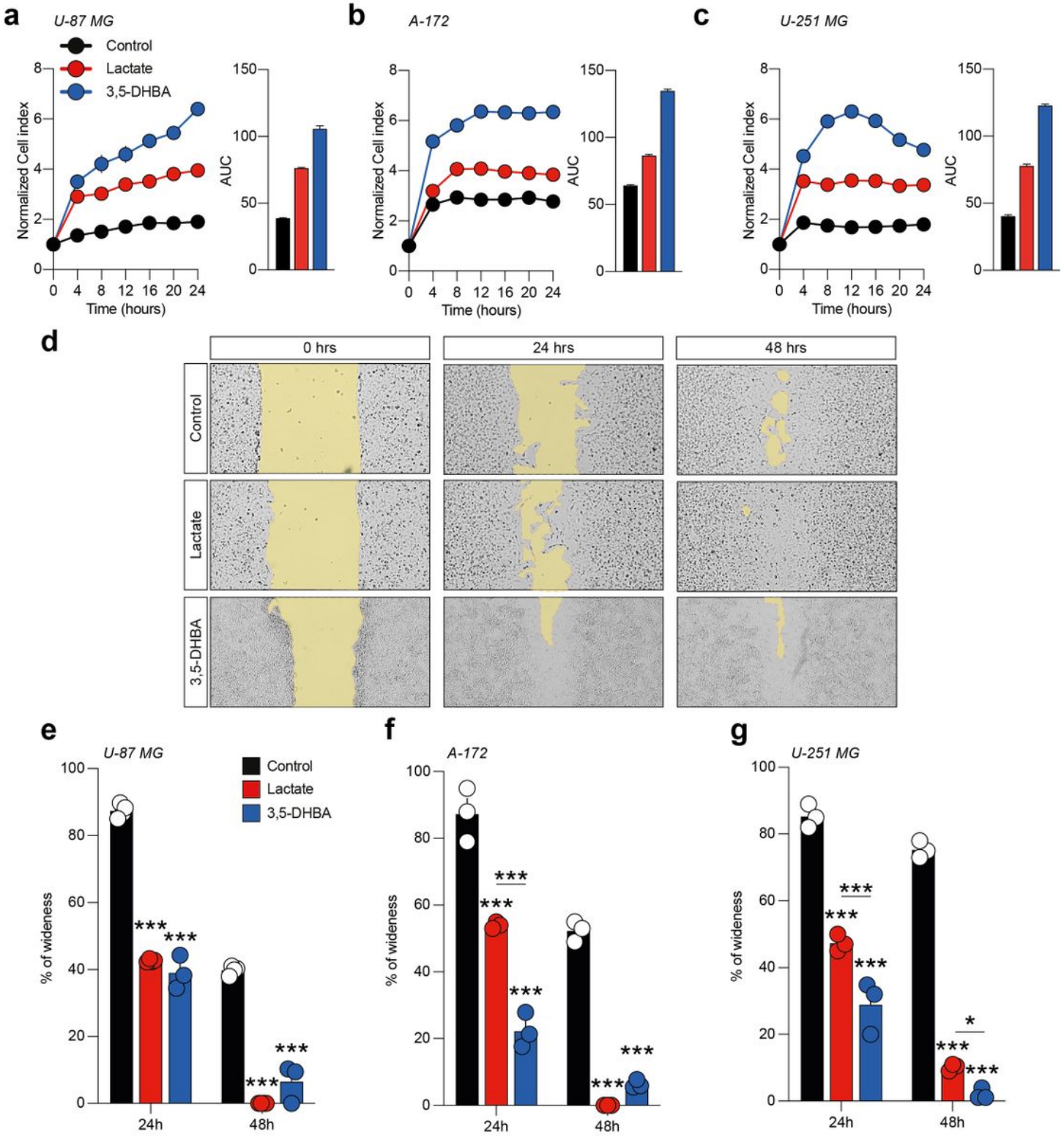

Figure 1

Lactate and 3,5-DHBA promote glioblastoma cell proliferation and migration Real-time cell proliferation monitoring by xCELLigence system following treatments with Lactate and 3,5-DHBA of U-87 MG cells (a), A-172 cells (b) and U-251 cells (c). Cell index values were normalized at the time of pharmacological treatments in order to obtain a normalized cell index. Each line is expressing the average of four different experiments. Analysis of human glioblastoma cell migration through a wound healing assay following

treatments of U-87 MG cells (e), A-172 cells (d-f) and U-251 MG cells (g) with Lactate and 3,5-DHBA. Figures presented are the representative of at least three independent experiments (means ± SEM). p values < 0.05 were considered to be statistically significant (*p < 0.05; **p < 0.01; ***p < 0.001).

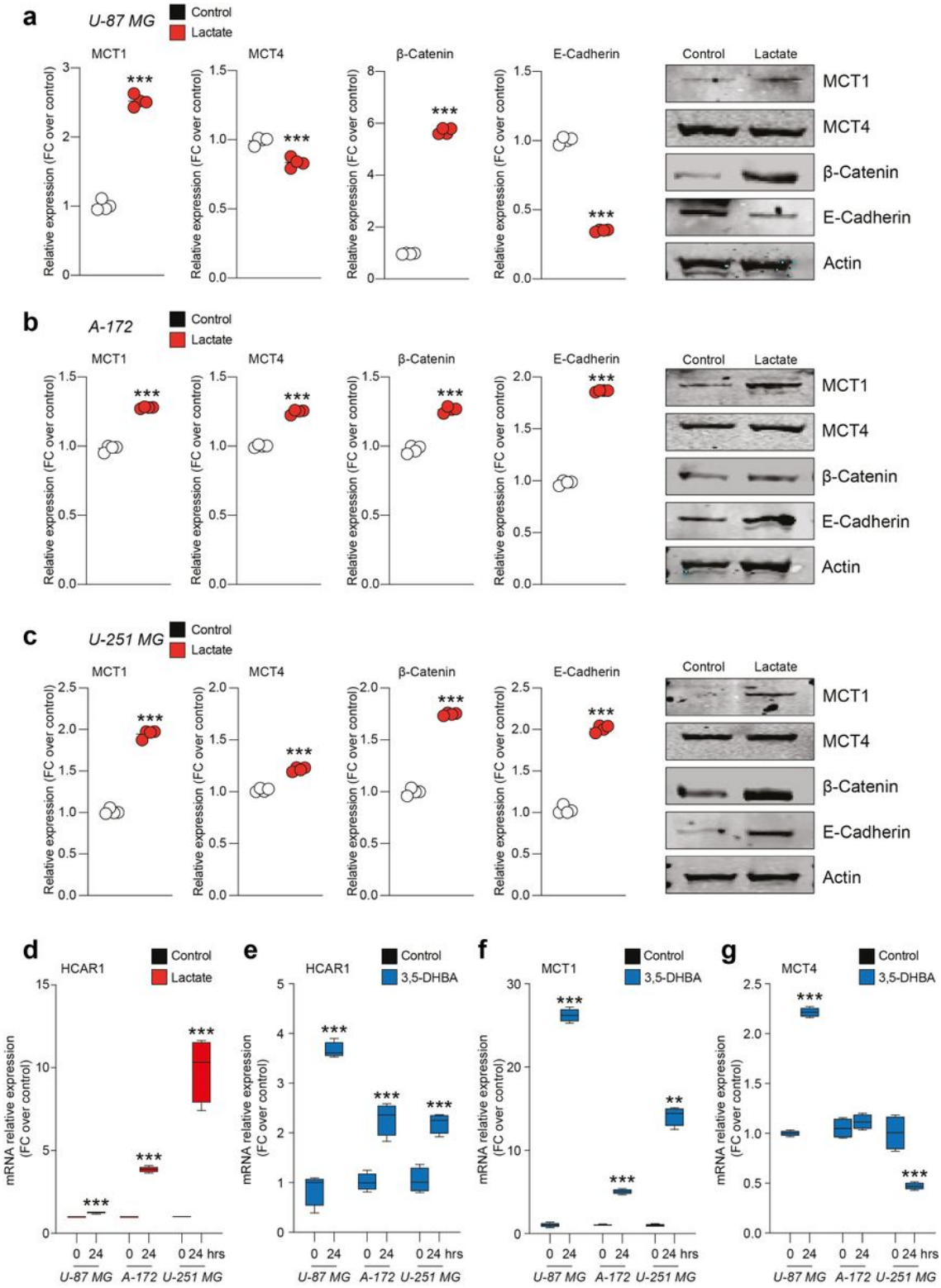

Figure 2

Lactate regulates the expression of MCTs and EMT markers in Glioblastoma cells. MCT1, MCT4, B-Catenin and E-Cadherin protein expression in U-87 MG cells (a), A-172 cells (b) and U-251 MG cells (c)

following 72 h of lactate treatment. Figures presented are the representative of at least four independent experiments and values represent the means ± SEM of experiments performed in quadrupled. HCAR1 gene expression (d) in U-87 MG, A-172 and U-251 MG cells following 24 h of lactate treatment. HCAR1 (e), MCT1 (f) and MCT4 (g) gene expression in U-87 MG, A172 and U-251 MG cells following 24 h of 3,5-DHBA treatment. Values represent the means ± SEM of experiments performed in quadrupled. p values < 0.05 were considered to be statistically significant (*p < 0.05; **p < 0.01; ***p < 0.001 vs untreated).

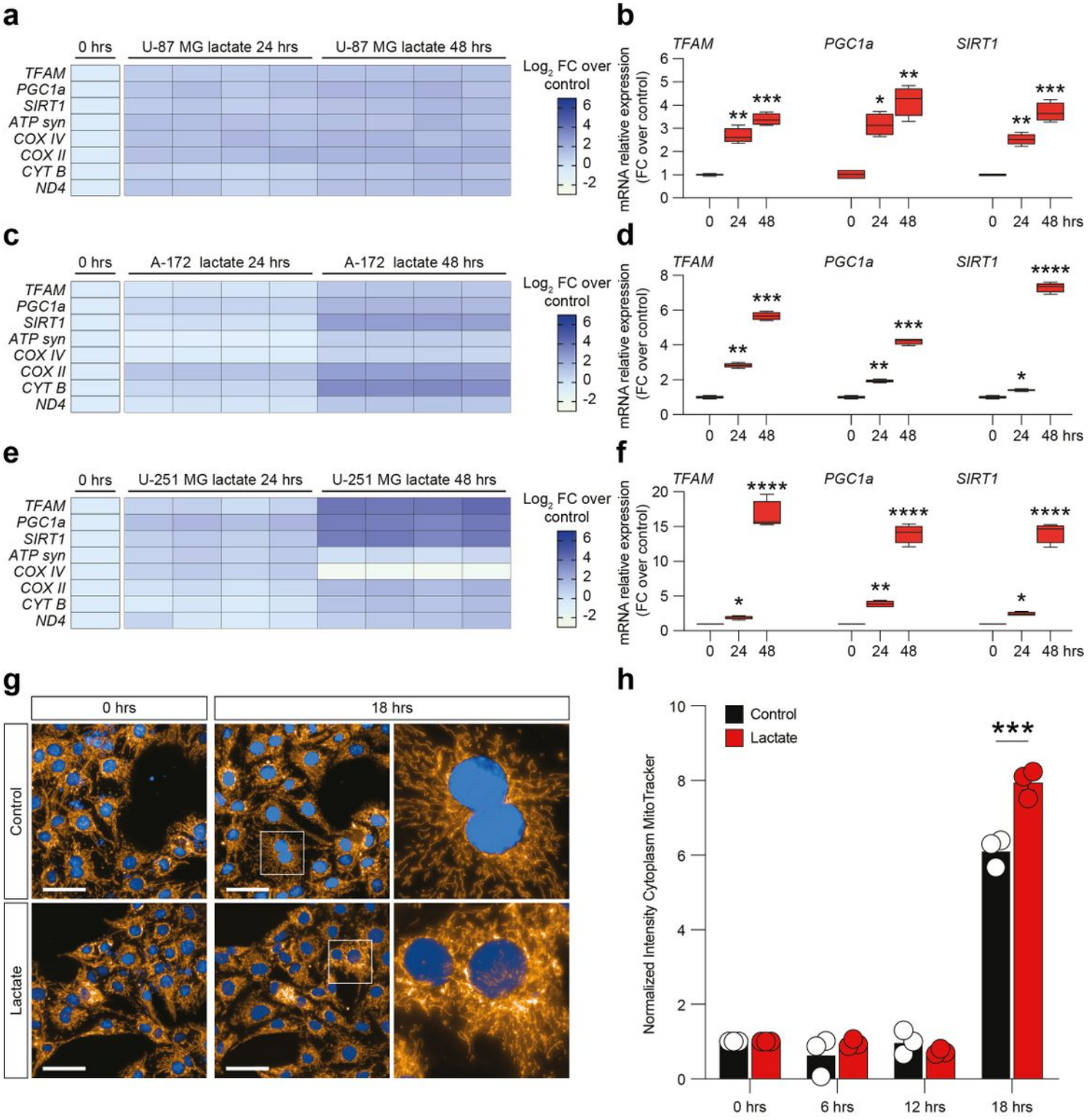

Figure 3

Lactate promotes up-regulation of Mitochondrial activity gene expression in Glioblastoma cells. Effect of Lactate on Mitochondrial biogenesis and OXPHOS gene expression in U-87 MG cells (a-b), A-172 cells (c-d) and U-251 MG cells (e-f) following 24 and 48 h of treatment. Computerized analysis of mitotracker fluorescence intensity on the control versus lactate 18 hours after treatment (g-h). Figures presented are the representative of at least three independent experiments. Values represent the means ± SEM of experiments performed in quadrupled. p values < 0.05 were considered to be statistically significant (*p < 0.05; **p < 0.01; ***p < 0.001 vs untreated).

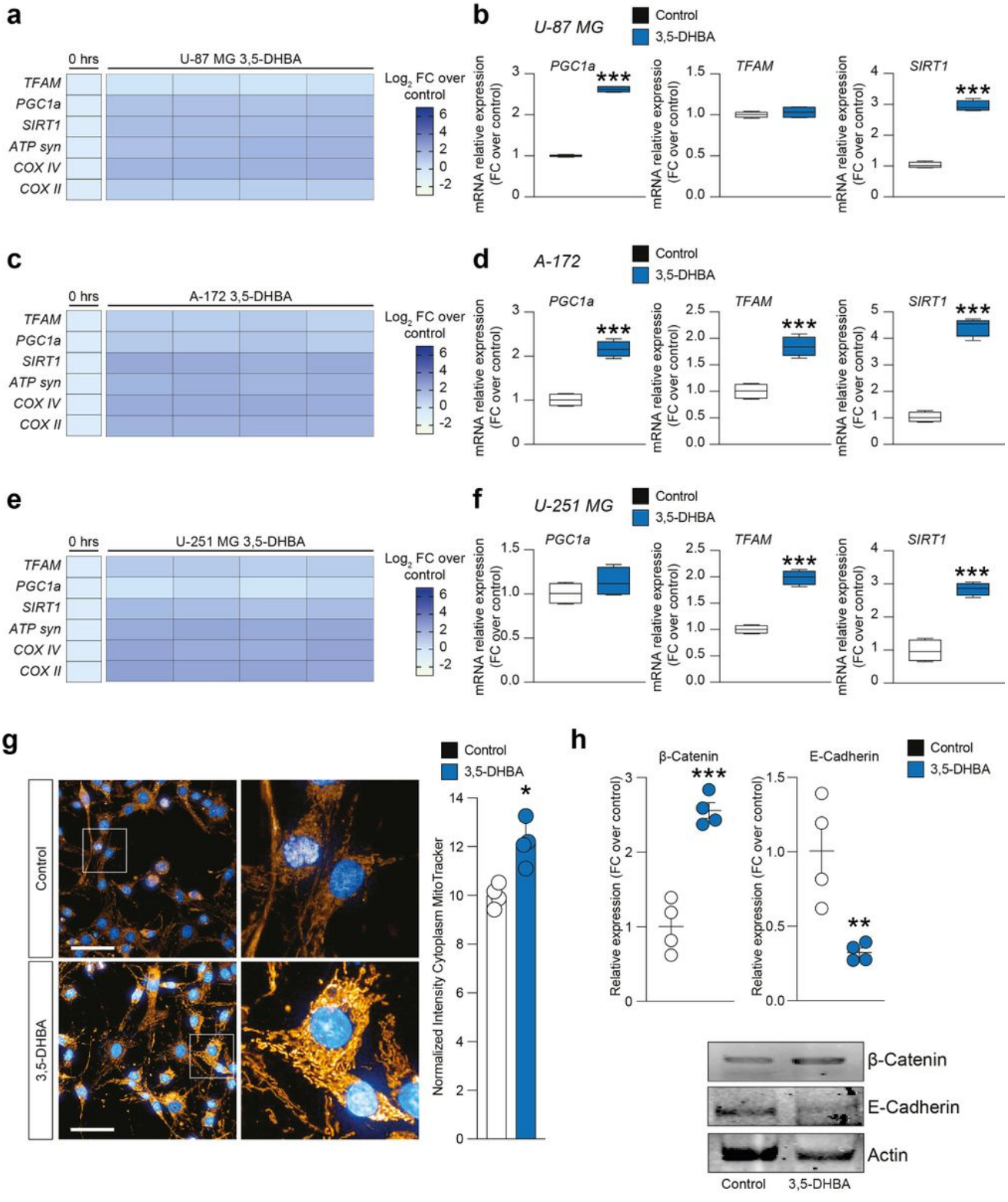

Figure 4

HCAR1 selective stimulation promotes up-regulation of Mitochondrial activity gene expression and regulates the protein expression of EMT markers in Glioblastoma cells. Effect of 3,5-DHBA on Mitochondrial biogenesis and OXPHOS gene expression in U-87 MG cells (a-b), A-172 cells (c-d) and U-251 MG cells (e-f) following 24 h of treatment. Computerized analysis of mitotracker fluorescence intensity on the control versus lactate 18 hours after treatment (g). Figures presented are the representative of at least three independent experiments. B-Catenin and E-Cadherin protein expression in A-172 cells (h) following 72 h of HCAR1 stimulation. Figures presented are the representative of at least four independent experiments and values represent the means ± SEM of experiments performed in quadrupled. p values < 0.05 were considered to be statistically significant (*p < 0.05; **p < 0.01; ***p < 0.001 vs untreated).

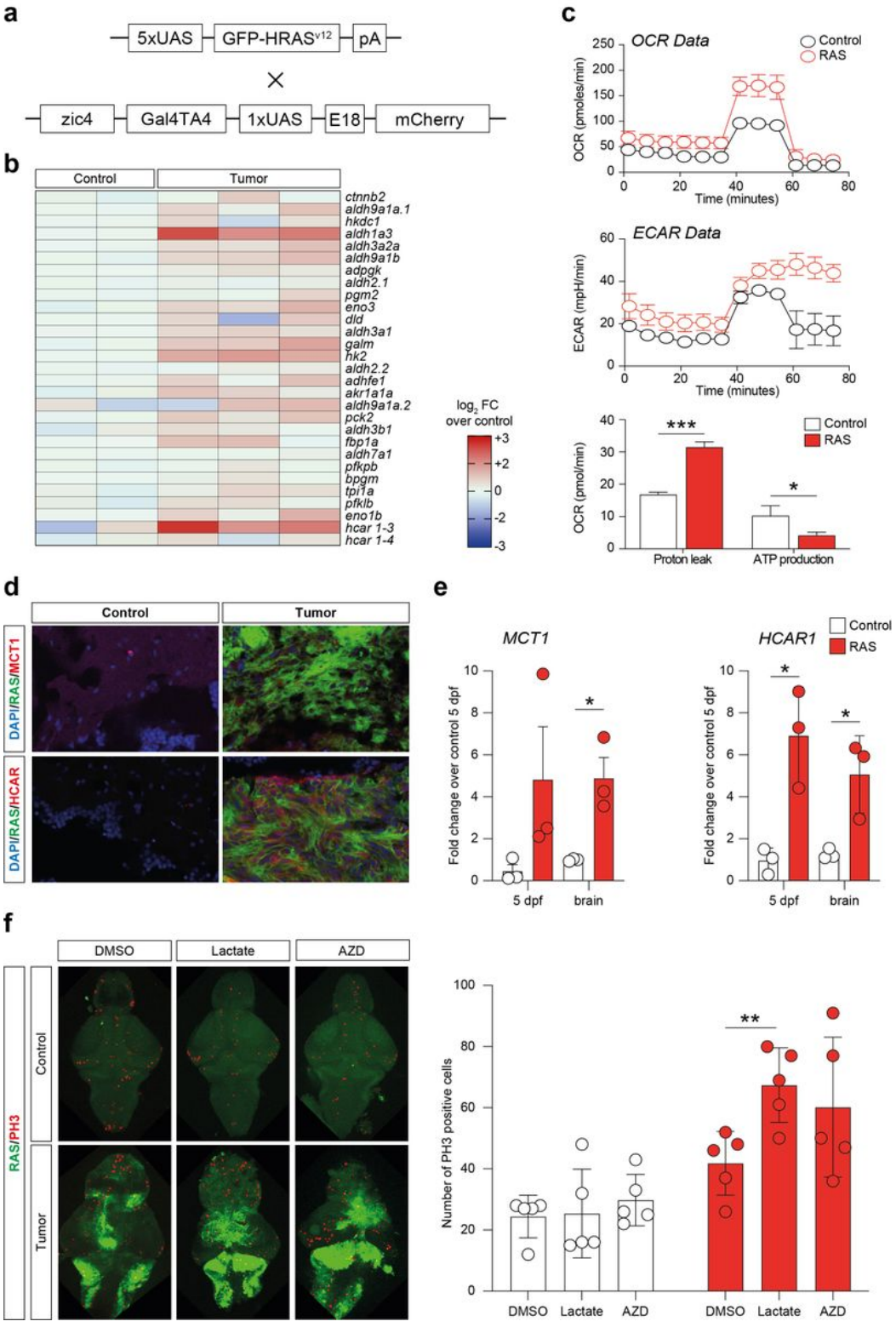

Figure 5

Metabolic changes in a zebrafish model of GBM leads to increased glycolysis and lactate transport and sensing. (a) schematic representation of the genetic components of the zebrafish GBM model (Mayrhofer et al., 2017); (b) increased expression of several members of the glycolytic pathway in GBM. Heatmap representing 29 glycolysis genes and their relative expression levels. (c) Analysis of mitochondrial metabolism (mitostress test) of tumor cells by XP Seahorse technology. d) Increased levels of HCAR1 in

tumors vs control as visualized by immunofluorescence. Staining as detailed in the figures, which are representative of at least 3 different experiments. (e) Gene expression analysis through q-PCR expressed as fold changes compared to controls, at 5dpf and in the adult tumors. Values represent the means ± SEM of experiments performed in triplicate. p values < 0.05 were considered to be statistically significant (*p < 0.05 vs controls). (f) Whole mounts immunofluorescence of Ph3 proliferating cells in controls and in HRAS overexpressing larvae treated or not with 20 um lactate. Green fluorescence represents tumoral cells expressing eGFP-HRASG12V. (g) number of proliferating cells in the brains treated as indicated.

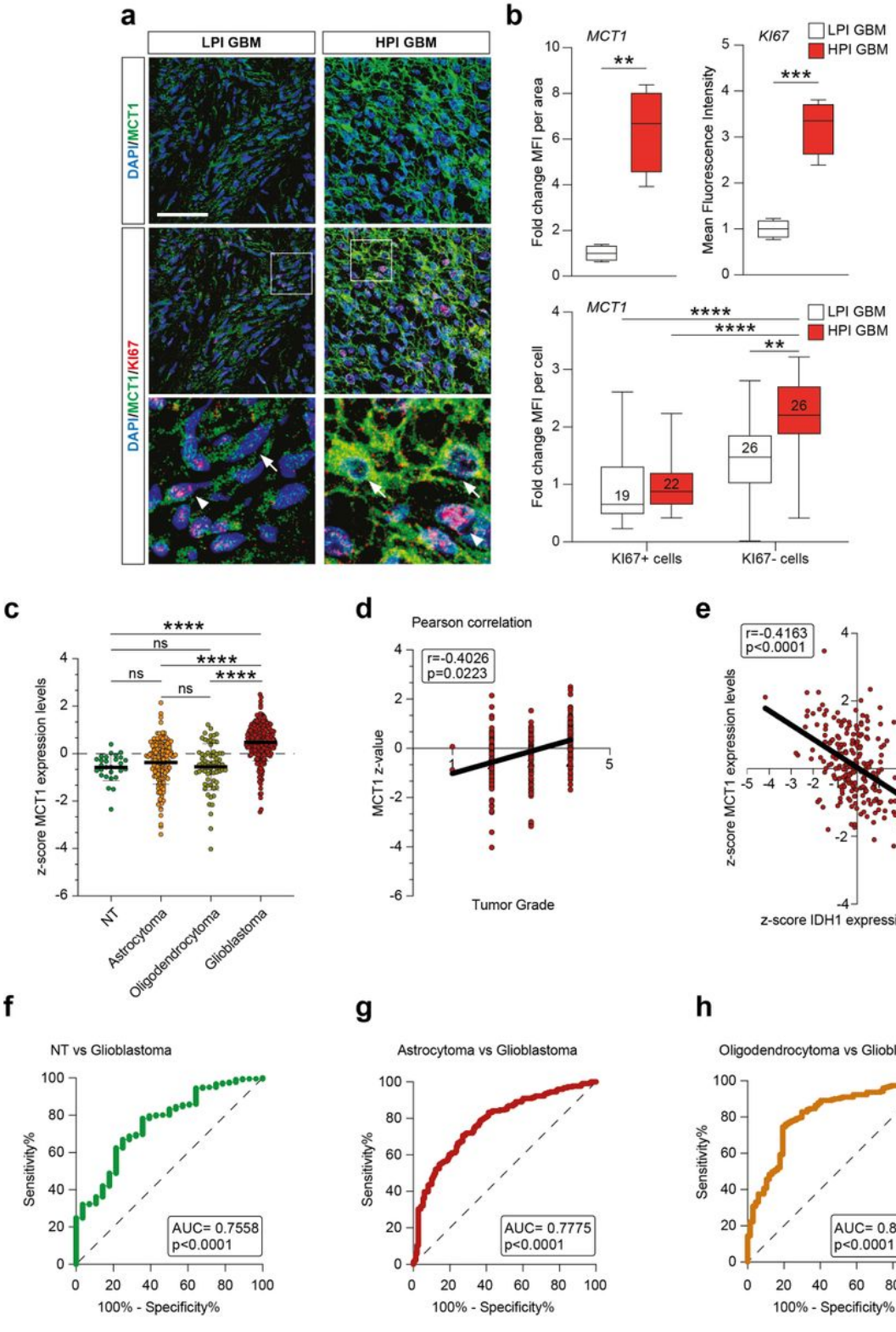

Figure 6

MCT1 expression analysis from the human brain tumor GSE108474 dataset Analysis of MCT1 gene expression in brain biopsies of patients with astrocytoma, oligodendrocytoma, glioblastoma, and healthy subjects. b) Pearson correlation analysis between MCT1 expression levels and tumor grade of brain biopsies obtained from patients affected by main brain tumors. c) Pearson's correlation between MCT1 and IDH1 expression levels in brain biopsies of patients with glioblastoma. d) Receiver operating characteristic (ROC) analysis between MCT1 brain expression levels in healthy subjects vs glioblastoma patients, between glioblastoma patients vs astrocytoma patients (e), and vs oligodendrocytoma (f). Data are expressed as mean ± SD of at least four independent experiments. (*p<0.05; **p<0.005; ***p<0.001; ****p<0.0001).

Supplementary Files

This is a list of supplementary files associated with this preprint. Click to download.

- FigureS1.jpg